TIME-REVERSAL MIRRORING FOR NEAR-ULTRASONIC INDOOR COMMUNICATION

Arthur Aubertin, Julien de Rosny, Pierre Jouvelot

TIME-REVERSAL MIRRORING FOR NEAR-ULTRASONIC INDOOR COMMUNICATION

Arthur Aubertin[1,2,3] **Julien de Rosny**[3] **Pierre Jouvelot**[2]
[1] Stimshop, 14-16 rue Soleillet, Paris, France
[2] MINES ParisTech, PSL University, Paris, France
[3] Institut Langevin, ESPCI Paris, PSL University, Paris, France
arthur.aubertin@mines-paristech.fr

ABSTRACT

We present the first use of a Time-Reversal Mirror (TRM) for near-ultrasonic indoor communication and discuss its advantages over existing techniques. For indoor applications where radio-frequency telecommunications are not suitable, acoustic solutions can indeed be a viable alternative. In this work, we experimentally evaluate the performance of a new acoustic communication system operating between the audible spectrum and near-ultrasounds, a range seldom studied for communication purposes. This choice allows us to take advantage of consumer transceivers while limiting users' hearing discomfort. To design a robust communication system and improve its overall bit rate, we combine a linear-frequency-modulation spread-spectrum technique and TRM. For testing purposes, we have developed a prototype array of speaker-microphones and implemented a TRM-based communication protocol. We first characterize this TRM device in an anechoic chamber. We then evaluate its focusing effectiveness in typical indoor environments and receiver-transmitter configurations. The quality of transmission is assessed via measurements of bit-error rates, with and without TRM, as a function of the signal-to-noise ratio. We also study how indirect paths impact communication robustness during changes in the environment. Finally, we present a concrete communication application between our TRM device and a consumer device, namely a smartphone.

1. INTRODUCTION

For many indoor applications, for instance when concerns over ATEX [1] hazards, electromagnetic disturbances, high privacy requirements, etc., exist, usual radio-frequency telecommunications may not be suitable. In such cases, acoustic solutions can represent an interesting alternative. Emerging startups such as Stimshop [2] already provide ultrasonic wireless communication systems and work to improve those systems.

In this work, we introduce and experimentally evaluate the performance of a new acoustic communication system operating between the audible spectrum (less than 17 kHz, say) and near-ultrasounds (about 17 to 25 kHz). This range of frequencies, rarely studied for communication purposes so far, allows to take advantage of a wide choice of transceivers developed for consumer applications while limiting the users' hearing discomfort.

More specifically, the communication system studied here combines a linear-frequency-modulation spread-spectrum technique, used to encode information and increase detection robustness, with a Time-Reversal Mirror (TRM) to spatially focus the signal message and thus improve the bit rate, necessarily Shannon-limited by our rather narrow frequency-band choice. To this end, we have developed a 40-cm-wide TRM made of 8 pairs of co-located speakers and electret microphones to communicate with user devices.

In addition to designing a simple analytical model of our system, we performed a series of experiments to assess the effectiveness of our proposed TRM-based approach. The TRM focusing efficiency in various typical environments (office, corridor, library) and configurations, namely line-of-sight (LOS) and non-line-of-sight (NLOS). Transmission quality is assessed via the measurement of Bit-Error Rates (BER), with and without TRM, as a function of the Signal-to-Noise Ratio (SNR). During focused emissions, we study the contribution of indirect paths on the communication robustness with changes in the environment or when the receiver is mobile. Finally, we present a concrete application case of communication between our TRM prototype and a consumer device, namely a smartphone. We study the impact of non-co-location of the speaker and the microphone on the focusing characteristics. This preliminary work shows the relevance and promising prospects of the use of TRM for acoustic indoor communications compared to other techniques.

Our main contributions are:

- an analytical BER model for audio communication and its generalisation to speaker arrays;
- the evaluation of near-ultrasound indoor communication effectiveness with multiple receivers over dedicated channels;
- the characterization of the effects and limits of non-co-located transmitter-receiver pairs in TRM-based processing.

This paper is structured as follows. Following this introduction, Section 2 provides an overview of the background

[1] ATEX Directive 2014/34/EU, for possibly explosive atmospheres
[2] http://www.stimshop.com

notions in acoustics and telecommunications required to better understand our approach. Then, Section 3 discusses related work. In Section 4, a simple BER model for acoustic communication is presented; we provide an analytical approximate model, its numerical validation and its generalisation to speaker arrays. Our experimental setup and TRM-based communication protocol are detailed in Section 5. Experiments, in LOS and NLOS configurations, are presented in Section 6; results and their relation to our model are discussed. Finally, Section 7 introduces an application ofe our TRM-based communication system to smartphones and shows the importance of co-located transmitter and receiver pairs. Section 8 concludes and introduces possible future work.

2. BACKGROUND

Since this work is at the intersection of several scientific disciplines, such as acoustics, electronics, signal processing and telecommunications, we present here an overview of the fundamental concepts that are frequently used in this paper (the knowledgeable reader can skip to the next section, after checking out our notations). We present linear chirps in Section 2.1, which we use to encode information, the basics of acoustic focusing and time-reversal mirroring in Section 2.2, a classification of communication configurations in Section 2.3, depending on the number of receivers and transmitters, and the concept of bit-error rate in Section 2.4, for telecommunication evaluation.

2.1 Linear chirp

To encode bits, we use a linear frequency modulation (or "chirp"), where the frequency of a sinusoidal signal varies between pulsations ω_0 and ω_1 (their absolute difference is $2\pi B$, where B is the frequency bandwidth) during a time interval, or "symbol-time", T. A bit 1 (resp. 0) corresponds to a frequency-increasing (resp. decreasing) chirp. The expression of a chirp $c(t)$ is given by

$$c(t) = A\sin(\varphi_n(t)), \tag{1}$$

$$\varphi_n(t) = n\frac{\pi B}{T}t^2 + \omega_0 t, \tag{2}$$

$$n = \frac{\omega_1 - \omega_0}{|\omega_1 - \omega_0|}, \tag{3}$$

where A is the amplitude of the chirp and time t ranges between 0 and T. In our system, an apodization Dirichlet window $D_{T,\alpha}(t)$ is applied to the chirps to mitigate the slides lobes when the autocorrelation chirp is worked out to recover the bit. Fig. 1 shows an example of a 1.75 s-long chirp ranging between 17 kHz and 20 kHz.

The use of spread-spectrum encoding makes linear chirps resilient to noise and Doppler effects. Hence, they are often used in radar technology.

2.2 Acoustic focusing with time-reversal mirror

An acoustic Time-Reversal Mirror (TRM) is made of an array of pairs of co-located loudspeakers and microphones.

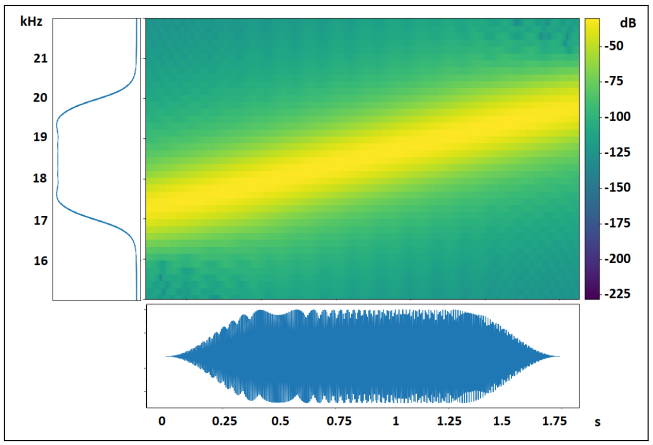

Figure 1. Linear chirp: time (bottom) and frequency (top) representations.

In a first step (a calibration step), a source emits a short pulse. The time-depend pressure field is recorded by each microphone of the TRM. In a second step, this set of impulse responses are flipped in time and sent back by each loudspeaker of the TRM. Thanks to the time reversal invariance, it has been shown that the acoustic wave back-propagates towards the initial source.

In free space, the focal spot presents an oblong shape (see Fig. 2). A TRM of width D focusing at a distance F produces a focal spot of length L and width l that are given by

$$L = 7\lambda\left(\frac{F}{D}\right)^2 \qquad \text{and} \qquad l = \lambda\frac{F}{D}, \tag{4}$$

where λ is the wavelength associated to the central frequency of the emitted signal.

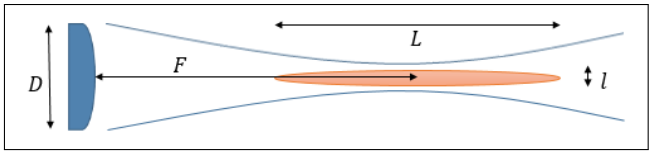

Figure 2. Acoustic focusing.

In a room, the geometry of the focus depends on the "critical distance". The critical distance is the distance from which the contribution of the indirect paths becomes stronger than the one due to the direct paths. When the distance between the TRM and the focus is smaller than the critical distance, the focus geometry is similar to free space one. On the contrary, when the distance between the TRM and the focus is larger, the field is diffuse and the focal spot becomes spherical with a typical diameter equals to half the wavelength (≈ 0.85 cm at 20 kHz in dry air).

2.3 Communication configurations

In telecommunications, the typical scheme consists of transmitting information between a transmitter, named Tx, and a receiver, named Rx. The transmitter and the receiver can be made of several elements. The type of configuration depends on the number of sources (or inputs) on the

Tx side and the number of probes (or outputs) on the Rx side. The main four configurations are: (1) single input - single output (SISO), (2) multiple inputs - single output (MISO), (3) single input - multiple outputs (SIMO) and (4) multiple inputs - multiple outputs (MIMO).

In the case of a transmitter sending independent user-specific information to multiple distinct receivers, the system is called "multi-user" (MU). Both transmitter and receiver could be made of one or multiple elements. Below, we focus on two particular configurations: MU-SISO and MU-MISO.

2.4 Bit-Error Rate

One of the most widely used tools to evaluate digital communication systems is the Bit-Error Rate (BER). It quantifies, statistically, the probability of an error occurring during the transmission of a bit (0 or 1). BERs can be estimated using several different methods, as presented in [1].

For this study, we compute BERs for various configurations as means of the error rates observed, by comparing the received bits with the expected ones, during the transmission of several random messages. Since detection is a binary choice, once the BER reaches 50%, the transmission is considered ineffective.

3. RELATED WORK

There has been a renewed interest in the use of airborne ultrasound communication, due to its advantages in comparison to radio-frequency (RF) communications for specific indoor applications. Near-ultrasound communication in the air allows simple implementations on various systems as Public Address (PA) or smartphones. As shown by Jiang and Wright in [2], Quadratic Amplitude Modulation (QAM) and Orthogonal Frequency-Division Multiplexing (OFDM), known and used for RF communications, can be applied to ultrasounds (around 40 kHz) to achieve high-rate data transmissions of up to 0.8 Mb/s, at 1.5 m. However, increasing the distance drastically reduces the bit rate, lowering it to 100 kb/s at 20 m.

In order to improve the robustness with respect to noises and Doppler effects, Lazik and Rowe, in [3], have proposed to use near-ultrasound linear chirps (around 20 kHz) to perform accurate indoor localisation to within 3 cm. Chirp compression, initially developed for RADAR systems can also be used to improve radio communications in low-SNR environments, as shown by Wang et al. in [4]. An application to SISO communication in near-ultrasounds has been developed by Stimshop.

The notion of TRM was developed by Fink and Prada in [5], then studied and adapted to the case of reverberant pieces by Yon et al. in [6]. Combining this method with phase-shift keying modulation, the feasibility of acoustic MISO and MIMO communications has been shown [6, 7]. Building upon this previous work, we propose to extend and check the practical viability of TRM for near-ultrasound communication. In practice, we quantify the efficiency of TRM-based communication in both reverberating rooms and other various indoor configurations, whether LOS or NLOS. We also apply this system to study the impact, for a given transceiver, namely a smartphone, of the non-co-location of its emitter (speaker) and receiver (microphone) in indoor TRM-based near-ultrasound communications.

4. BER MODEL

Chirp modulation belongs to the family of spread-spectrum coding that provides a strong resistance to noise. We present here an analytical model of the BER-vs-SNR relationship for various chirp lengths.

4.1 SISO approach

We code bits 1 and 0 as linear chirps that use the same pulsation boundaries ω_0 and ω_1, but just swapped; they are noted $c_n(t)$, with n given by Eqn. (3). To detect the increasing or decreasing chirps in a signal, this last is correlated, i.e., match filtered, with these 2 predefined chirps. We assume that the signal received $y(t)$ is the sum of a noise $w(t)$, for which the noise spectrum power density p is supposed constant across the bandwidth B, and the symbol, i.e., one chirp $c_m(t)$, of amplitude A.

$$y(t) = Ac_m(t) + w(t). \tag{5}$$

The correlation S_{mn} of the signal received with a test chirp $c_n(t)$ is given by

$$S_{mn} = AC_{mn} + \int_{-\infty}^{+\infty} w(t)c_n(t)\mathrm{d}t, \tag{6}$$

where C_{nm} is the correlation of chirp $c_n(t)$ with $c_m(t)$. The BER r that is defined as the probability of wrong bit detection can be expressed in terms of the probability of correlation comparison

$$r = P(S_{n'n} > S_{nn}), \tag{7}$$

which is also given by

$$r = P(S_{n'n} - S_{nn} > 0). \tag{8}$$

With the hypothesis of $S_{nn'}$ and S_{nn} being Gaussian variables, simple computations lead to an exact BER formulation

$$r = \frac{1}{2}\mathrm{erfc}\left[\frac{A\sqrt{C_{nn} - C_{n'n}}}{2\sqrt{p}}\right], \tag{9}$$

where erfc is the complementary error function.

A numerical integration of the C_{nm} integrals provides the results given in Fig. 3, for different symbol-times T, at a sample rate of 88.2 kHz. The model suggests that, as expected, the longer the chirps are, the more resistant to noise detection is.

To provide in-silico validation of this BER model, we performed a computer simulation of 1-bit communications, using 50k iterations for each SNR point, assuming the presence of "white" noise. The simulation results, shown in Fig. 4, match quite closely the analytical model.

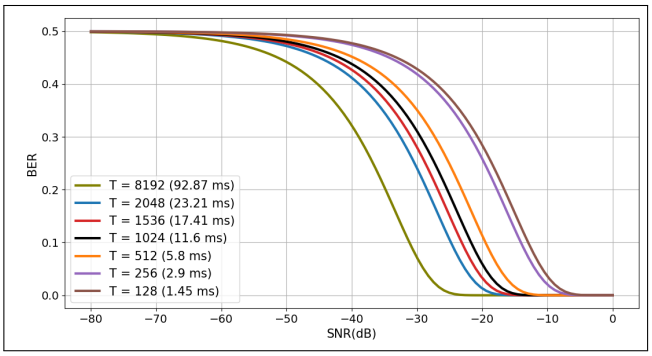

Figure 3. SISO BER model (analytical).

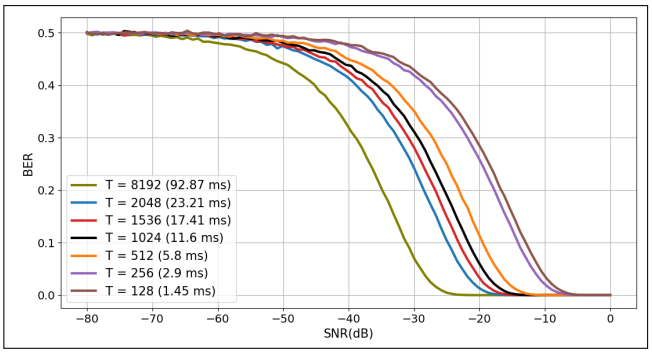

Figure 4. SISO BER model (simulation).

4.2 MISO generalization

In order to extend the previous BER model to array systems of (multiple) transmitters, we introduce an approximate model parameterised over the number N of array elements.

First, the inter-correlation term in the root square of Eqn. (9) is neglected, while the autocorrelation is approximated to the one of a truncated sine function:

$$\sqrt{C_{nn} - C_{nn'}} \approx \sqrt{C_{nn}} \approx \sqrt{\frac{T}{2}}. \tag{10}$$

Then, as the noise power density p is constant on the whole spectrum, the noise spectrum power over the bandwidth B is:

$$P_B = p \int_B \mathrm{d}f = pB. \tag{11}$$

Using Eqn. (10) and Eqn. (11) and assuming that time-reversal focusing enhances the received amplitude by a factor N, an approximate expression of the BER r is given by

$$\mathrm{r} \approx \frac{1}{2}\mathrm{erfc}\left[\frac{1}{2}\sqrt{\frac{(NA)^2}{2P_B}}\sqrt{BT}\right]. \tag{12}$$

This formulation introduces the typical BT term, often present when discussing communication performance. Fig. 5 shows instances of Eqn. (12) for an array of $N = 8$ elements; a gain of approximately 15 dB is brought by the presence of these multiple transmitters.

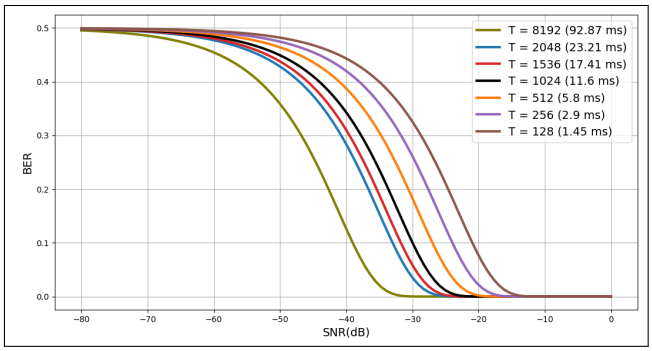

Figure 5. MISO BER model for $N = 8$ speakers.

5. EXPERIMENTAL SETUP AND PROTOCOL

An experimental setup has been designed and implemented to assess the performance of Time Reversal and MU-MISO communications.

5.1 Transceivers and array

We designed and built a custom-made transceiver with a Dayton Audio loudspeaker ND16FA-6 (33-mm diameter, 10 W), mounted on a custom-made 3D printed enclosure, and a small electret microphone (4-mm diameter) in front of it, at its center, fixed with a vertical nylon thread (see Fig. 6). The loudspeaker can be connected via an RCA connector, and the microphone, via a 3.5-mm jack. This assembly is called a "mono-element" in the rest of the paper.

The microphone is connected to a custom-made electret-mic phantom power source and to a RME preamplifier Octamic II. The loudspeaker is connected to a custom-made amplifier.

Up to 10 mono-elements can be accessed synchronously via an AD/DA sound card Orion 32+. The sound card is connected to a computer.

Figure 6. Experimental transceiver.

A 40-cm-wide time-reversal mirror, made of a linear array of 8 mono-elements, is mounted on a stand as shown in Fig. 7. Two mono-elements (Rx1 and Rx2) are typically facing the time-reversal mirror. A microphone mounted on a translation axis can probe the field over one axis.

All the audio equipment being in a rack, the setup can be easily moved. A mono-element and the entire array have been characterised in an anechoic chamber at Sorbonne

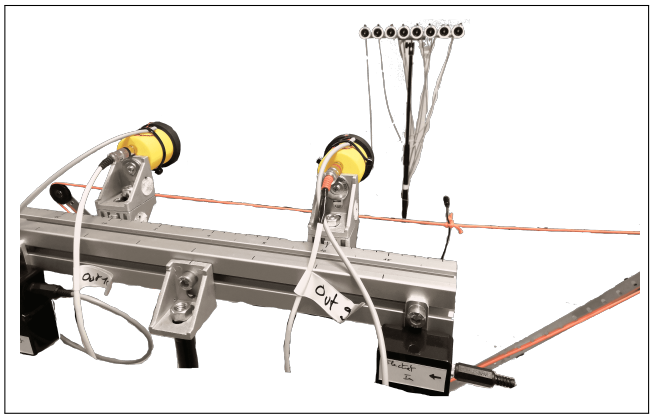

Figure 7. Experimental transceiver and array.

University. Directivity diagrams show a large opening at -3 dB, around 60 degrees, in reception and emission.

5.2 Experimental protocol

5.2.1 Indoor configurations

The experimental measurements have been performed indoor at Langevin Institute in three different places. First, the system is set up in a closed room, as shown in Fig. 8, for LOS configurations.

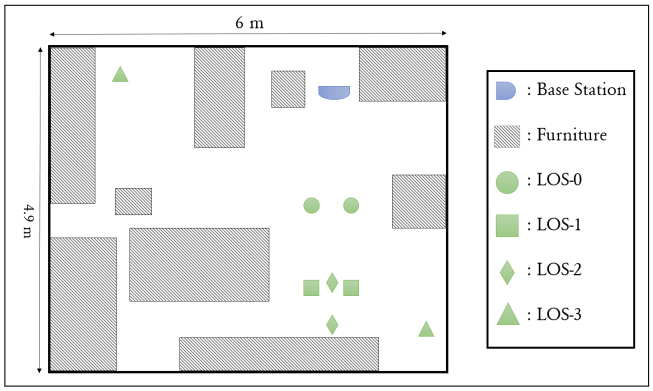

Figure 8. Closed-room configurations.

Then, the system is set up in a corridor and a library for further LOS and NLOS configurations, as shown in Fig. 9.

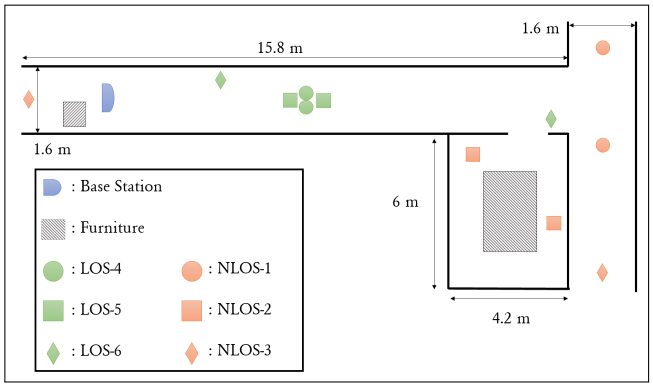

Figure 9. LOS (corridor) and NLOS (corridor and library) configurations.

5.2.2 Measurement protocol

As seen before, a time-reversal process starts by a calibration phase where the impulse responses (IR) between the TRM and the two mono-elements have to be acquired. The typical way consists of emitting a calibration signal (a chirp) successively from the two mono-elements and recording the responses on the 8 microphones of the TRM. We also implemented the reciprocal method, where a calibration signal is emitted successively from each array element and the responses are recorded simultaneously on the two mono-elements.

Then, the IRs are computed by cross-correlating the responses with the source calibration signal and flipped in time. To transmit a message to a specific mono-element, its content is convoluted with the time-reversed IR (TRIR) between this mono-element and the TRM. To achieve MU-MISO communication, the signals generated to focus on each mono-element are summed before transmission.

Finally, the received focused signals are processed for data extraction: correlation energies are compared to identify the slope of the incoming chirps and, thus, decode the sent information.

6. MU-MISO EXPERIMENTS

This section presents the experimental results obtained with TRM in the LOS and NLOS configurations specified above.

All recorded signals are sampled at a rate of 88.2 kHz, and a long chirp followed by 5 chirp symbols are sent for communication (5-bit messages). The long chirp is used for pre-detection and synchronisation before decoding the 5-chirp thread. Chirps with a bandwidth of 1 kHz, a central frequency of 18.5 kHz and a length of 1536 samples are used.

6.1 LOS configurations

6.1.1 Acoustic focusing

First, we show the differences introduced by the type of communication, in the LOS-0 configuration, where an up-chirp and a down-chirp are respectively focused on Rx1 and Rx2. For SISO and MU-MISO, the chirps are sent simultaneously, while sent successively for MISO on Rx1 and MISO on Rx2. In Fig. 10, for each receiver and for each type of communication, the two correlations with an up-chirp and and a down-chirp are given.

In the SISO case, Rx1 and Rx2 received the two chirps equally, as shown by the superposed and very similar correlation results. Thus it is not possible to decode successfully the expected signal on each receiver.

TRM-based MISO emissions show that the focusing is there correctly performed. The expected chirp-compression effect is well visible on the aimed Rx, while chirp compressions on the other Rx are very low. This suggests that the focal spot is well concentrated around the target point. This behaviour is the same for MISO on Rx1 and on Rx2.

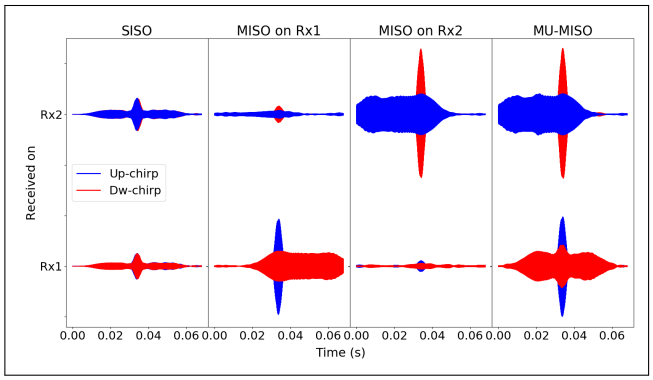

Figure 10. Focusing comparison between SISO, MISO and MU-MISO in LOS-0.

In the MU-MISO configuration, the up- and down-chirps are focused simultaneously on Rx1 and Rx2, respectively. For each Rx, the expected chirp-compression effect is visible and distinct from the other one. However, as focusing is performed simultaneously on both receivers, the spurious chirp-compression effect on Rx1 has increased in comparison to the "pure" MISO-on-Rx1 results. The MU part of the communication protocol tends to diminish chirp compression gaps.

In order to quantify the focal spot width, the perpendicular field is measured with a microphone mounted on a 1-axis translation bench (see Fig. 7). Fig. 11 displays the energy on a Rx and on the mobile microphone. The focal spot size is consistent with the expected one, as discussed in Section 2. Indeed, in LOS-0, for $F \approx 1.72$ m, Eqn. (4) gives $l \approx 7.3$ cm, while the experimental focal spot width, evaluated with the width of the received energy at mid-height, is $l_{exp} \approx 7.29$ cm.

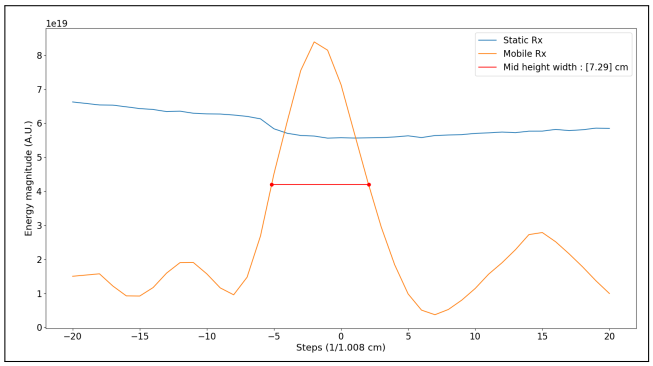

Figure 11. Focal spot measurement for LOS-0.

6.1.2 Communications

For each configuration, random data frames are sent 100 times. SNRs are computed, with the maximum of the received signal as reference. The tables below show averaged SNRs and BERs on Rxs.

The LOS-0 configuration, in Tab. 1 is the reference; its proximity from the TRM explains its strong SNR and a flawless communication decoding. As expected, for LOS-1, the energy decreases, as the Rx-TRM distance increases,

Config.	LOS-0	LOS-1	LOS-2	LOS-3
	Rx1 - Rx2	Rx1 - Rx2	Rx1 - Rx2	Rx1 - Rx2
SNR_{dB}	56 - 60	53 - 58	64 - 59	46 - 36
$\text{BER}_{\%}$	0. - 0.	0. - 0.	9.8 - 18.6	0. - 0.

Table 1. Room LOS communication results

and even more, for LOS-3, where this distance keeps growing, and Rx2 is in a diffuse field. The alignment of Rxs in the LOS-2 configuration leads to a superposition of focal spots, hence the SNRs gain. However, this mixing causes confusion for decoding.

Tab. 2 shows that, in a very reflecting area, Rxs receive more energy from indirect paths. In the LOS-5 case, the field is diffuse and focal spots do not superpose, the diameter of the focal spot spot being way smaller than the inter-Rxs distance. The TRM also manages to focus on two points with a large gap between them (LOS-6).

Config.	LOS-4	LOS-5	LOS-6
	Rx1 - Rx2	Rx1 - Rx2	Rx1 - Rx2
SNR_{dB}	71 - 63	69 - 66	57 - 71
$\text{BER}_{\%}$	0. - 0.	0. - 0.	0. - 0.

Table 2. Corridor LOS communication results

6.2 NLOS configurations

6.2.1 Acoustic focusing

First, as in Section 6.1, SISO and MU-MISO configurations are compared. Fig. 12 shows chirp-compression effects. The received energy has decreased in both cases. Indeed, in NLOS, only indirect paths contribute to the focusing, and multiple reflections attenuate the energy. The SISO SNR is too low to allow proper detection.

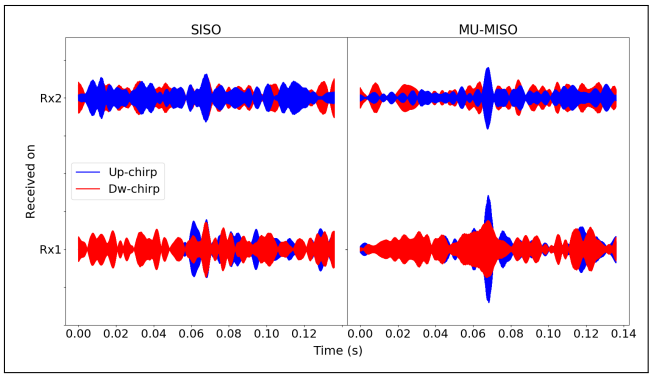

Figure 12. Focusing comparison between SISO and MU-MISO in NLOS-2.

6.2.2 Communications

The communication process uses the same parameters as in Section 6.1, and the results are shown in Tab. 3. Even with a significant loss of SNR compared to LOS configurations

(between -40 dB and -15 dB), the decoding is successful for NLOS-2 and NLOS-3. In the case of NLOS-1, further measurements have shown that this is due to grating lobes and focal spot superposition. The focal spot's small diameter in a diffuse field allows to kill this effect by moving Rx2 a few centimeters away, dropping the BER to 0.

Config.	NLOS-1	NLOS-2	NLOS-3
	Rx1 - Rx2	Rx1 - Rx2	Rx1 - Rx2
SNR_{dB}	31 - 30	31 - 29	39 - 25
$BER_{\%}$	0.6 - 21.6	0. - 0.	0.2 - 0.

Table 3. NLOS communication results.

6.3 Discussion

As shown previously, our TRM enables LOS and NLOS indoor communications, simultaneously on two receivers. Results are broadly consistent with our BER model (see Fig. 5), since positive SNRs lead to perfect communications ($r = 0$). However, the model does not consider the surrounding elements, induced by MU-MISO communications.

Placing Rxs around a grating lobe from another one or aligning them represent limits of this TRM, liable to a BER rise. To prevent grating lobes errors, the pre-detection chirp of the focused signal could be signed, up or down.

By introducing non-linear forms of chirps with logistic or polynomial frequency functions, i.e., with S-shaped instantaneous frequency curves and their $\pi/2$ rotations, we could have up to 6 receivers with their unique pre-detection id.

7. SMARTPHONE APPLICATION

In this section, our TRM communication system is applied to a smartphone, to achieve MISO communications.

7.1 Experimental setup

The challenge, here, is the non-co-location of the speaker and microphones in smartphones, in this case a Honor Play running Android 9. The main microphone (MM) is located near the speaker, at about 7.5 mm, i.e., half the typical wavelength of our signals. The second microphone, i.e., the camera or ambient microphone (AM), is located far from the speaker, on the other side of the phone, at about 16.8 cm (see Fig. 13).

This disposition allows two ways of performing calibration: (1) with the bi-directional calibration (BC), the smartphone sends the calibration signal; (2) with the unidirectional calibration (UC), the TRM sends the calibration. For UCs, a synchronisation step is necessary to synchronise clocks: the signal received by the smartphone must be properly re-sampled. A local Wi-Fi network is used to retrieve the signal received by the smartphone, send it commands and centralise all computations on the computer.

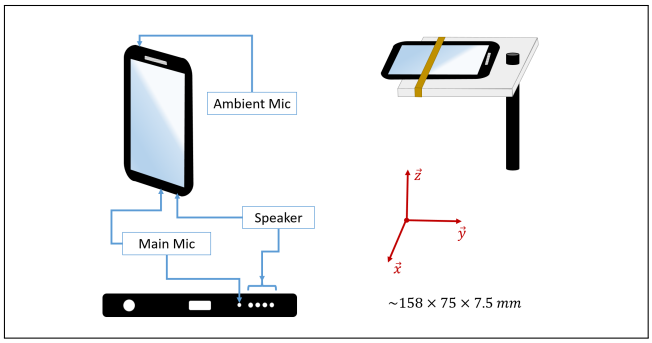

Figure 13. Smartphone.

The measurements are made in the same room, corridor and library as before. The smartphone is placed face up on a plate, mounted on a microphone stand. To prevent the local network stream processing between the computer and the smartphone from disrupting the communication, via potential slowness and data loss, the sample rate is lowered to 44.1 kHz. Hence chirps have a length of 768 samples, while keeping their bandwidth and central frequency.

7.2 MISO experiments

To start, the linearity of the signals focused on the smartphone and the stationary condition of the smartphone resampling have been verified.

7.2.1 Acoustic focusing

The smartphone orientation on the focus plan is relevant in near field. Two positions are considered: perpendicular (Pos1) and parallel (Pos2) to the TRM. Fig. 14 shows the focusing in LOS-1 for the two positions, depending on the calibration method and the receiving microphone.

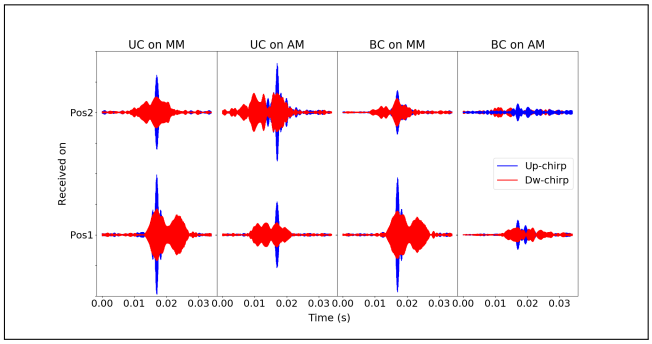

Figure 14. LOS-1 focusings on the smartphone.

In Pos1 and BC, the AM profits of the focal-spot length, while in Pos2 and BC, it does not overflow on both microphones. For Pos2 and BC, energy losses are visible, due to the orientation of the microphones and their sensibilities.

Fig. 15 presents the LOS-3 results, i.e., in diffuse field. The focal-spot geometry allows a clean chirp compression in UC. The non-co-location of the speaker and the MM induces a loss of energy in BC.

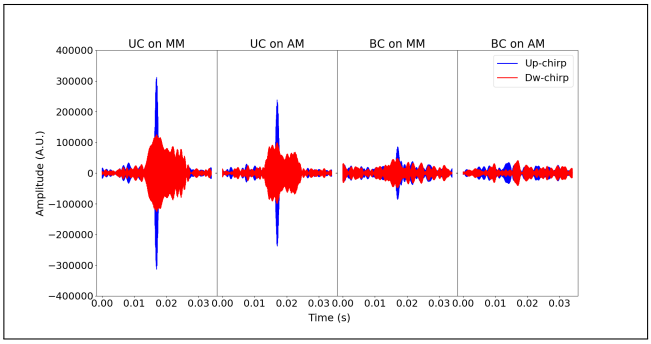

Figure 15. LOS-4 focusings on the smartphone.

7.2.2 Communications

In order to keep the experimental time reasonable, random frames, with the same structure as in Section 6, are sent 20 times.

Fig. 16 shows averaged BER results in LOS-1 (Pos1 and Pos2) and LOS-3 for an UC and a BC on each microphone. For UC, the communication is perfectly performed, while for BC it is degraded.

In LOS-1, the BER is similar for MM and AM, around 25 %, due to the smartphone position. When focal spots do not cover both microphones or in a diffuse field, like in LOS-1 Pos2 and LOS-3, the MM BER is around 25 % - 30 %, which indicates a medium/low quality communication channel, while the AM BER, around 50 %, shows ineffective communications.

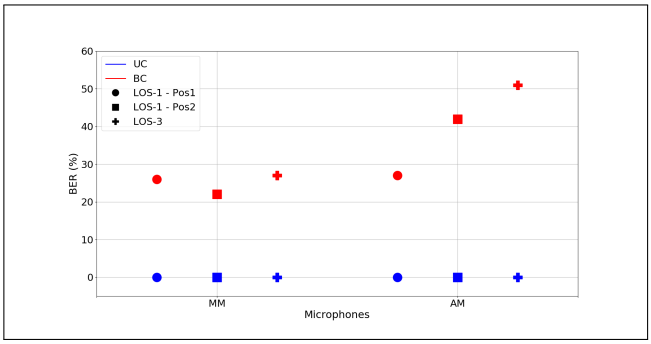

Figure 16. MISO smartphone BERs.

7.3 Discussion

This application to smartphones shows the great relevance of the distance between the microphone and the speaker of a receiver for a TRM system. As this distance grows (MM to AM reception), the communication degrades and the BER increases.

It is also clear, in the case of a BC calibration, that the speaker characteristics of the aimed receiver play an important role in the communication quality. Indeed, a precise and proper calibration allows to evaluate correctly the propagation channel, leading to accurate focusings.

In comparison to the results of Fig. 5, the BER loss from UC to BC, due the non-co-location of the speaker and the microphone, corresponds to a SNR loss of at least $\sim$12 dB.

8. CONCLUSION

A BER model for TRM-based near-ultrasonic indoor communication has been presented, and its approximation for speaker arrays of N-elements has been elaborated.

An experimental 8-mono-element TRM with two mono-element receivers has been detailed and setting up in many indoor configurations in order to evaluate near-ultrasound MU-MISO communications and their limits.

An application of the TRM with a smartphone has been detailed to highlight the impact of a receiver with non-co-located speaker and microphone.

For future work, we intend to further validate our BER model and extend these MISO experiments with the smartphone in NLOS configurations.

Acknowledgements

We thank Jean-Loïc Le Carrou (LAM, Jean Le Rond d'Alembert Institute, Sorbonne University) for providing us access to the Jean Le Rond d'Alembert Institute anechoic chamber. We thank Cédric Coppin for electronic advice and his contributions to the manufacturing of the custom amp and pre-amp in our experimental setup.

9. REFERENCES

[1] J. Dong, *Estimation of Bit Error Rate of any Digital Communication System*. PhD thesis, Télécom Bretagne, 2013.

[2] W. Jiang and W. Wright, "Full-duplex airborne ultrasonic data communication using a pilot-aided QAM-OFDM modulation scheme," *IEEE Transactions on Ultrasonics, Ferroelectrics, and Frequency Control*, vol. 63, pp. 1–1, 05 2016.

[3] P. Lazik and A. Rowe, "Indoor pseudo-ranging of mobile devices using ultrasonic chirps," in *Proceedings of the 10th ACM Conference on Embedded Network Sensor Systems*, SenSys '12, (New York, NY, USA), p. 99–112, Association for Computing Machinery, 2012.

[4] J. Wang, S. Su, and Z. Chen, "Parameter estimation of chirp signal under low snr," *Science China Information Sciences*, vol. 58, pp. 1–13, 02 2015.

[5] M. Fink and C. Prada, "Acoustic time-reversal mirror," *Inverse Problems J.*, vol. 17, 02 2001.

[6] S. Yon, C. Dorme, and M. Fink, "Sound focusing in reverberating rooms: The time-reversal approach," *Journal of the Acoustical Society of America*, vol. 105, pp. 934–934, 02 1999.

[7] J. Candy, A. Meyer, A. Poggio, and B. Guidry, "Time-reversal processing for an acoustic communications experiment in a highly reverberant environment," *Journal of The Acoustical Society of America*, vol. 115, p. 1621, 2004.